

Folded Textured Sheets

Mark SCHENK*, Simon D. GUEST

Department of Engineering, University of Cambridge
Trumpington Street, Cambridge, CB2 1PZ, UK

* ms652@cam.ac.uk

Abstract

By introducing a ‘local’ texture to thin-walled sheets, the ‘global’ mechanical properties of the sheets can be favourably modified. In this paper we explore the intriguing mechanical properties of Folded Textured Sheets, by way of two examples. The fold patterns allow the sheets to undergo large deformations, as well as change their global Gaussian curvature without stretching the material. Furthermore, both example sheets share the remarkable property that their Poisson’s ratio under bending is of opposite sign to that under extension. The properties of the sheets were studied using a simple numerical model, where the folded sheets are represented by a pin-jointed framework; this captures the key deformation modes.

1. Introduction

In this paper we shall describe some of the novel and unique mechanical properties that have been observed in two example Folded Textured Sheets – see Figure 1. The qualitative description of the behaviour of the folded paper models is supported by the results from a simple numerical model. The most intriguing and counterintuitive property is that for both sheets their Poisson’s ratio under bending is of opposite sign to that under stretching. It is, however, primarily their ability to undergo large shape changes without stretching at material level, which suggests applications in morphing structures (*e.g.*, Thill et al. [8]).

The Folded Textured Sheets discussed in this paper form part of ongoing research into the properties and applications of textured sheets. By introducing a ‘local’ texture (such as corrugations, dimples, folds, etc.) to otherwise isotropic thin-walled sheets, the ‘global’ mechanical properties of the sheets can be favourably modified. The ‘local’ texture has no clearly defined scale, but lies somewhere between the material and the structural level and in effect forms a microstructure. A classic example is corrugated sheets, where the sheets’ bending stiffness is greatly increased at minimal expense of material and weight. Texture patterns have also been used to introduce geometrical anisotropy in order to create bistable behaviour in cylindrical shells (Norman et al. [4]). In Folded Textured Sheets the local texture is created by means of a tessellated fold pattern, inspired by the Japanese art of Origami folding. However, the sheets we are studying are not necessarily developable (*i.e.*, folded from a single sheet), but are generally characterised by a faceted, polyhedral surface.

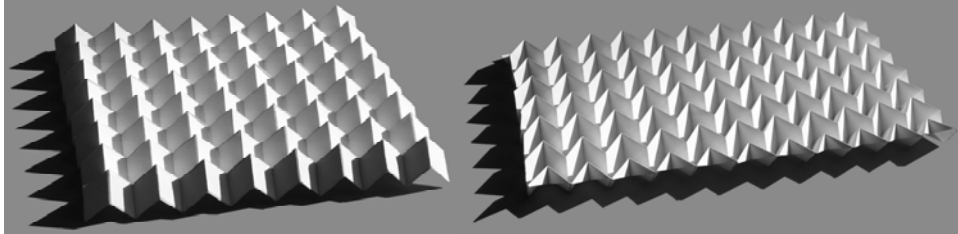


Figure 1: photographs of the Eggbox (left) and the Miura sheet (right). The models are made of standard printing paper, and the parallelograms in both sheets have sides of 15mm and an acute angle of 60° . The Miura sheet is folded from a single flat sheet of paper; the Eggbox sheet, in contrast, is made by gluing together strips of paper, and has an angular defect at its apices and saddle points.

2. Mechanical Properties

The first obvious property of the folded sheets is their ability to undergo relatively large deformations, by virtue of the folds opening and closing. Moreover, the fold patterns enable the sheets to locally expand and contract – and thereby change their global Gaussian curvature – without any stretching at material level. Gaussian curvature is an intrinsic measure of the curvature at a point on a surface, which remains invariant when bending, but not stretching the surface (Huffman [1]). Our interest lies with the macroscopic behaviour of the sheets, and we therefore consider the ‘global’ Gaussian curvature of an equivalent mid-surface of the folded sheet. Both the Eggbox and Miura sheets are initially flat, and thus have a zero global Gaussian curvature. Now, unlike conventional sheets, both folded textured sheets can easily be twisted into a saddle-shaped configuration which has a globally negative Gaussian curvature – see Figure 2(a) and Figure 3(a).

The sheets’ most intriguing property, however, relates to their Poisson’s ratio. Both sheets have a single in-plane mechanism whereby the facets do not bend and the folds behave as hinges; by contrast, facet bending is necessary for the out-of-plane deformations. As shown in Figure 2(b) and Figure 3(b), the Eggbox and the Miura sheet respectively have a positive and a negative Poisson’s ratio in their planar deformation mode. A negative Poisson’s ratio is fairly uncommon, but can for instance be found in foams with a reentrant microstructure (Lakes [2]). Conventionally, materials with a positive Poisson’s ratio will deform anticlastically under bending (*i.e.*, into a saddle-shape) and materials with a negative Poisson’s ratio will deform synclastically into a spherical shape. As illustrated in Figure 2(c) and Figure 3(c), however, both folded textured sheets behave exactly opposite to what is conventionally expected, and their Poisson’s ratio is of opposite sign for in-plane stretching and out-of-plane bending. This remarkable mechanical behaviour was previously only described theoretically for auxetic composite laminates (Lim [3]), but is here observed in textured sheets made of conventional materials.

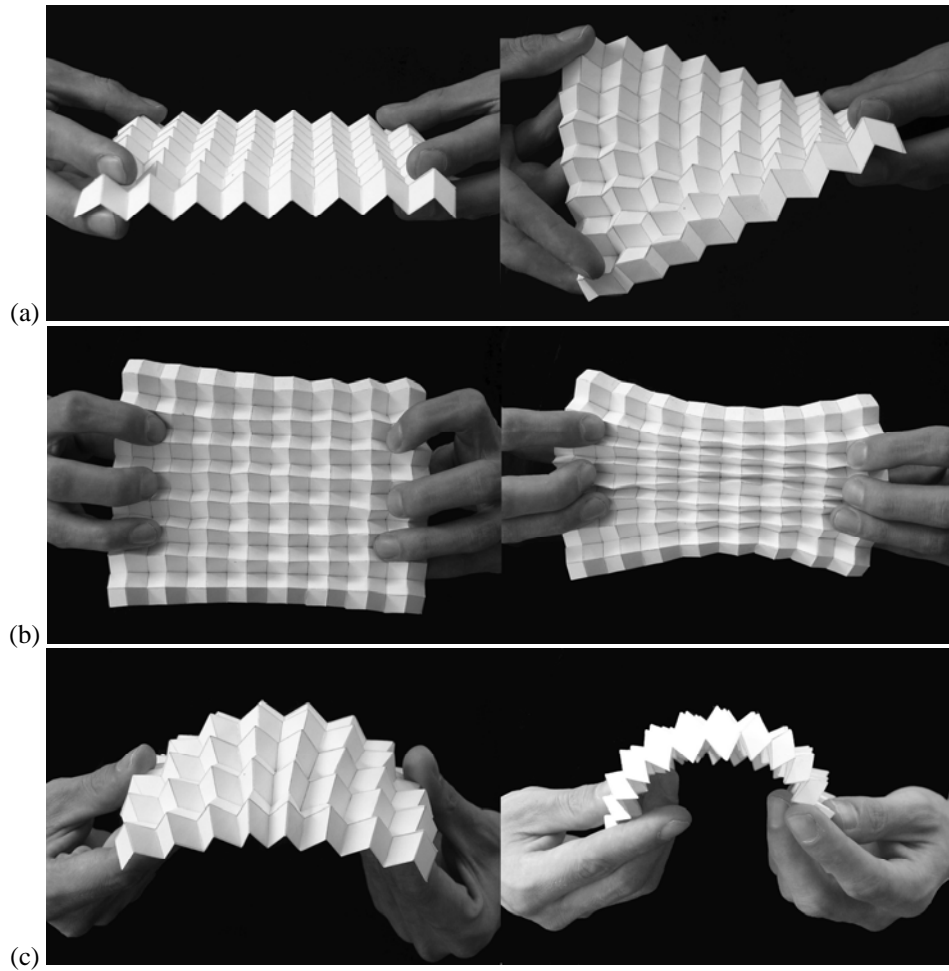


Figure 2: mechanical behaviour of the Eggbox sheet. Firstly, it can change its global Gaussian curvature by twisting into a saddle-shaped configuration (a). Secondly, the Eggbox sheet displays a positive Poisson's ratio under extension (b), but deforms either into a cylindrical or a spherical shape under bending (c). The spherical shape is conventionally seen in materials with a negative Poisson's ratio.

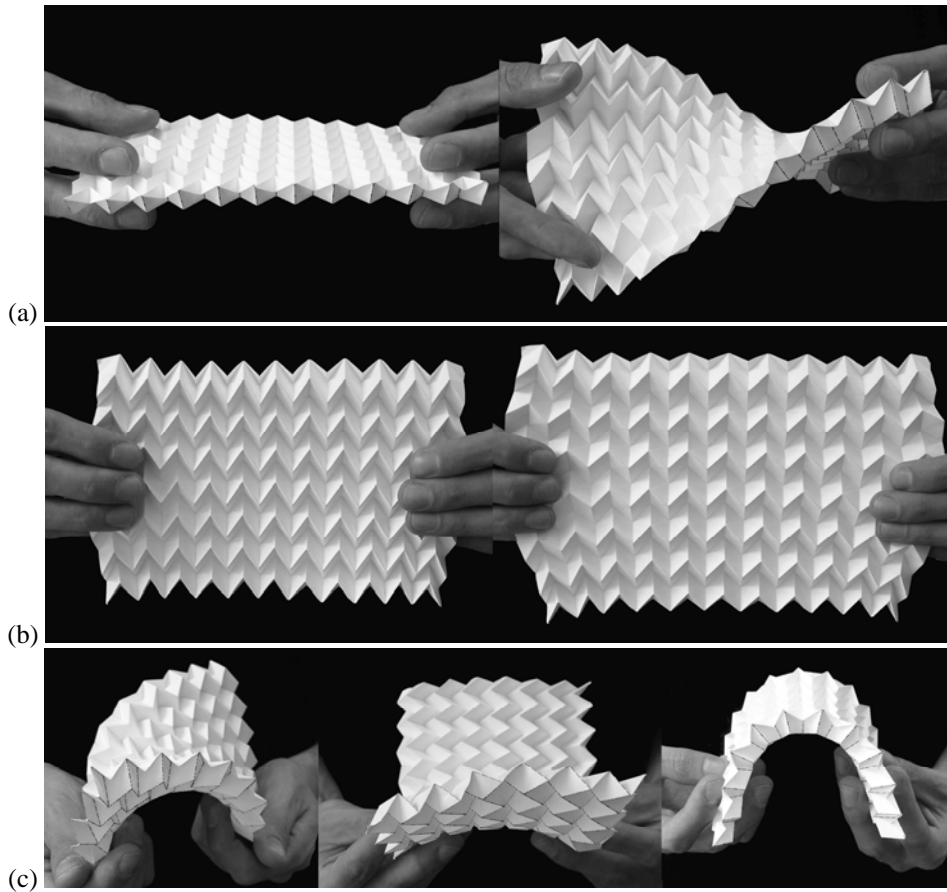


Figure 3: mechanical behaviour of the Miura sheet; it can be twisted into a saddle-shaped configuration with a negative global Gaussian curvature (a). Secondly, the Miura sheet behaves as an auxetic material (negative Poisson's ratio) in planar deformation (b), but it assumes a saddle-shaped configuration under bending (c), which is typical behaviour for materials with a positive Poisson's ratio.

3. Numerical Modelling

The folded textured sheets are modelled as pin-jointed frameworks (Figure 4), where bars and pin-joints respectively represent fold lines and vertices in the crease pattern. Furthermore, the fold pattern is triangulated to avoid trivial internal mechanisms, and to provide a first-order approximation for bending of the parallelogram facets. This simple approach provides insight in the global deformation kinematics of the sheet, without dealing with the minutiae of the stress distributions (Tanizawa and Miura [7]).

Once an equivalent bar framework has been set up, established structural analysis methods can be used to analyse the properties of the sheets (*e.g.* Pellegrino and Calladine [5]). The compatibility matrix \mathbf{C} is the Jacobian of quadratic bar length constraints, and relates the nodal displacements $\mathbf{d} = [d_x^1 d_y^1 d_z^1 \dots d_x^n d_y^n d_z^n]^T$ to the bar elongations $\mathbf{e} = [e_1 \dots e_m]^T$

$$\mathbf{C}\mathbf{d} = \mathbf{e} \quad (1)$$

The nullspace of the compatibility matrix, modulo rigid-body motions, provides the inextensional internal mechanisms of the structure. Planarity constraints between adjoining facets may also be added, by means of the Jacobian matrix \mathbf{J} that relates nodal displacements \mathbf{d} to changes in the dihedral angle $d\theta$ between two facets:

$$\mathbf{J}\mathbf{d} = d\theta \quad (2)$$

The constraints are combined into the augmented compatibility matrix $\tilde{\mathbf{C}} = [\mathbf{C}; \mathbf{J}]$, whose nullspace contains the planar deformation modes of the folded sheets; these involve no bar elongations or bending of the parallelogram facets. To give insight into the out-of-plane kinematics, the tangent stiffness matrix of the framework is used; since no pre-stress is considered, this is given by

$$\mathbf{K}_t = \tilde{\mathbf{C}}^T \mathbf{G} \tilde{\mathbf{C}} \quad (3)$$

where \mathbf{G} is a diagonal matrix with the axial member stiffness for the bars, and the bending stiffness between two constrained facets (either across the parallelograms, or along fold lines). An important parameter in modelling the sheets is the ratio between the bending

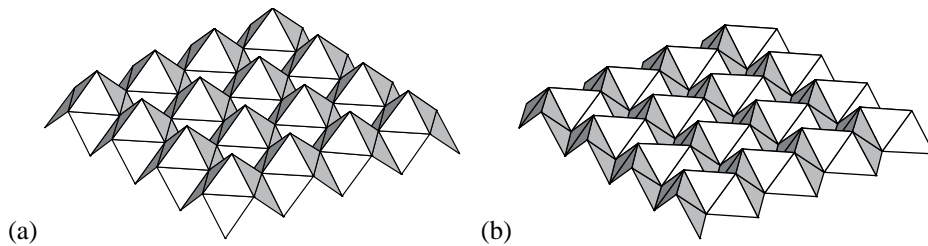


Figure 4: pin-jointed framework model of the Eggbox (a) and Miura (b) sheet. For both folded sheets a grid of 4×4 unit cells was used for the numerical analysis. The Eggbox sheet is in its square configuration, and the fold depth of the Miura sheet is determined by the 55° dihedral angle between the sheet's mid-plane and the facets.

stiffness of the parallelograms, K_{facet} , and the bending stiffness along the fold lines, K_{fold} . When the ratio $K_{\text{facet}} / K_{\text{fold}} \rightarrow \infty$ the facets become infinitely rigid, approximating the situation where the facets are connected through hinges; when $K_{\text{facet}} / K_{\text{fold}} \rightarrow 0$ the fold lines become rigid, which approximates a situation where the sheets are formed from a rigid flat sheet. For the paper models a value of $K_{\text{facet}} / K_{\text{fold}} = 1$ was estimated.

Plotting the mode shapes for the lowest eigenvalues of the tangent stiffness matrix provides insight into the deformation kinematics of the sheets. Of main interest are the deformation modes that involve no bar elongations (*i.e.*, no stretching of the material), but only bending of the facets and along fold lines. These modes are numerically separated by choosing the axial members stiffness of the bars to be several orders of magnitude larger than the bending stiffness for the facets and folds. A more rigorous separation could be achieved by orthogonalising the eigenmodes to the rowspace of the compatibility matrix, but in practice this did not prove necessary. In our analysis only first-order infinitesimal modes within \mathbf{K}_t are considered, and no iterative techniques are used to find large displacements.

The results of the numerical analysis of the Eggbox and Miura sheet are summarized in Figure 5 and Figure 6. The simple numerical model successfully captures the key mechanical behaviour observed in the paper models, and the counterintuitive out-of-plane deformation modes are among the softest (and therefore most dominant) eigenmodes of the tangent stiffness matrix \mathbf{K}_t . Importantly, these interesting modes remain dominant over a large range of values for $K_{\text{facet}} / K_{\text{fold}}$, which indicates that the behaviour is primarily a result of geometry and not the precise material properties. As expected, the single planar mechanism found in the nullspace of the augmented compatibility matrix $\tilde{\mathbf{C}}$ (*i.e.*, no bending of the facets) becomes the dominant mode as the ratio of $K_{\text{facet}} / K_{\text{fold}}$ increases.

4. Conclusions & Future Work

As illustrated by two example sheets, folded textured sheets display novel and interesting mechanical properties. They can undergo relatively large deformations as well as changes in their global Gaussian curvature, by virtue of the opening and closing of the folds. Both sheets also display the remarkable property that their Poisson's ratio under bending is of opposite sign to that under stretching. For instance, the Miura sheet displays auxetic behaviour in planar deformation, but deforms into a saddle shape under bending.

This paper represents the results of our initial studies of the properties of folded textured sheets. Their properties are yet to be fully understood, and future work will in part focus on establishing an equivalent continuum model for the sheets, as well as finding efficient production methods, to allow these unique sheets to be used in engineering applications such as morphing structures, where their novel mechanical properties provide new opportunities.

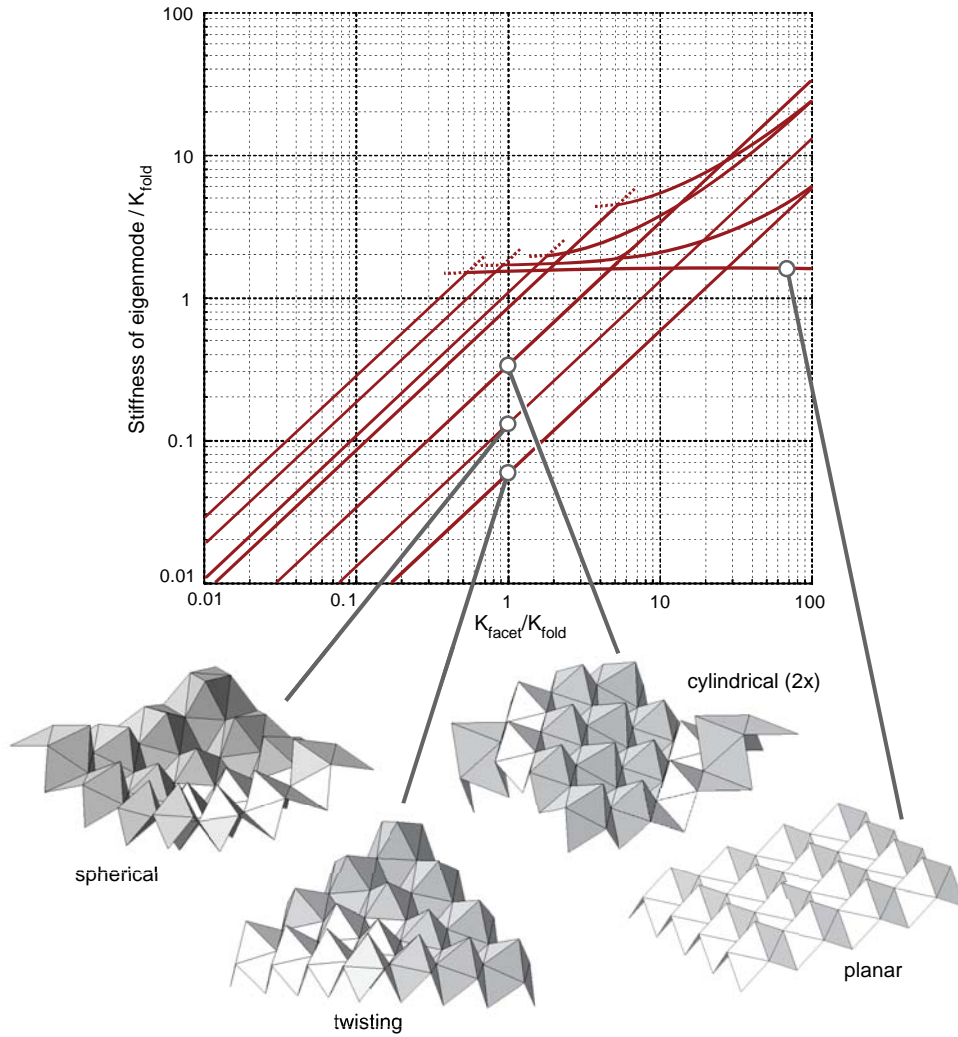


Figure 5: here is plotted the relative stiffness of the nine softest eigenmodes of the Eggbox sheet, as a function of the ratio $K_{\text{facet}} / K_{\text{fold}}$. It can be seen that the twisting, spherical and cylindrical deformations observed in the paper models remain the dominant mode shapes for a large range of configurations. They are eventually surpassed by the planar mechanism at $K_{\text{facet}} / K_{\text{fold}} \approx 27$.

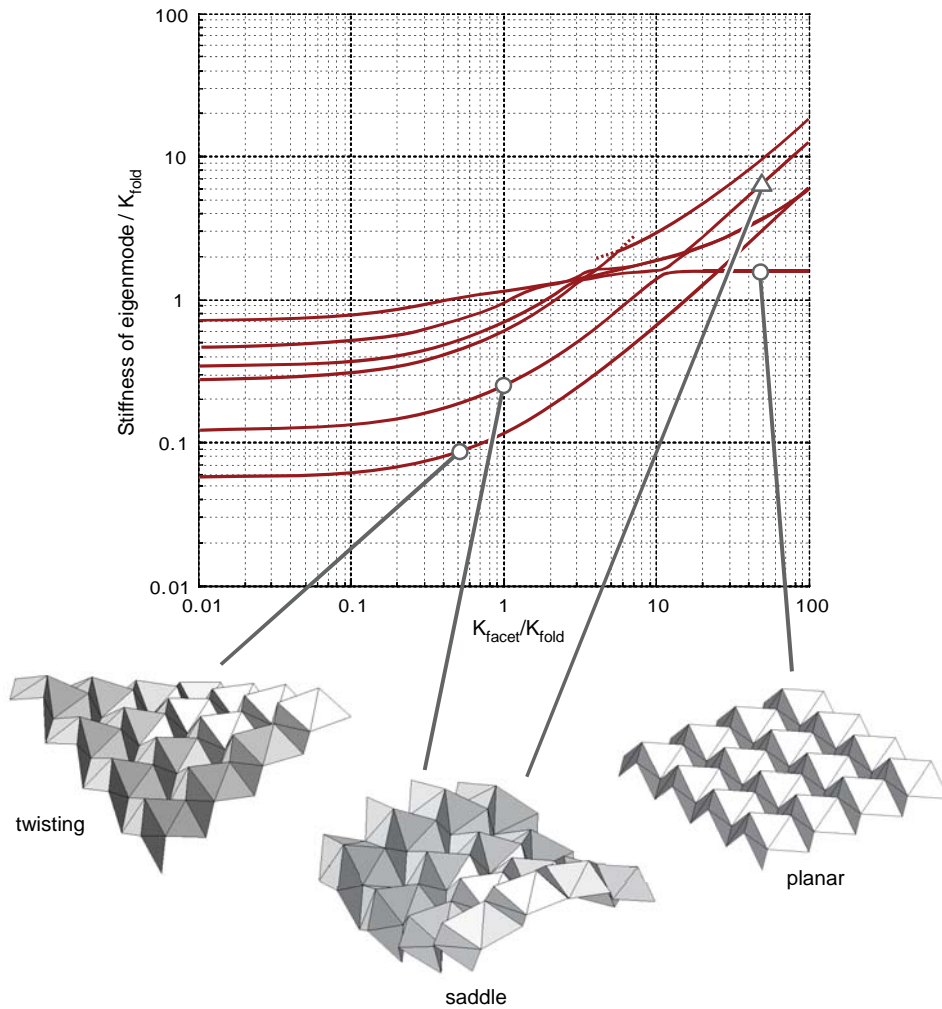


Figure 6: here is plotted the relative stiffness of the six softest eigenmodes of the Miura sheet. The twisting and saddle-shaped modes observed in the paper models are the dominant modes over a large range of configurations. At $K_{\text{facet}} / K_{\text{fold}} \approx 11$ the eigenvalue curve for the saddle-shaped mode abruptly veers, and its eigenmode undergoes a rapid (but continuous) change in shape: it flattens out into the planar mechanism, while another mode transforms into the saddle-shaped configuration. This ‘curve veering’ behaviour in eigenvalue curves indicates a coupling between the eigenmodes; in the limit case of zero modal coupling, the two eigenvalue curves cross (Perkins and Mote [6]).

Acknowledgements

MS gratefully acknowledges support from the EPSRC and Cambridge European Trust.

References

- [1] Huffman D.A., Curvatures and Creases: A Primer on Paper. *IEEE Transactions on Computers*, 1976; **C-25**; 1010-1019.
- [2] Lakes R., Foam Structures with a Negative Poisson's Ratio. *Science*, 1987; **235**; 1038 - 1040.
- [3] Lim T., On simultaneous positive and negative Poisson's ratio laminates. *Physica Status Solidi (b) Solid State Physics*, 2007; **244**; 910 - 918.
- [4] Norman A.D., Golabchi M.R., Seffen K.A. and Guest S.D., Multistable Textured Shell Structures, *CIMTEC 2008*, Acireale, Sicily, Italy: 2008.
- [5] Pellegrino S. and Calladine C.R., Matrix analysis of statically and kinematically indeterminate frameworks. *International Journal of Solids and Structures*, 1986; **22**; 409–428.
- [6] Perkins N.C. and Mote C.D., Comments on curve veering in eigenvalue problems. *Journal of Sound and Vibration*; **106**; 451-463.
- [7] Tanizawa K. and Miura K., Stress Analysis of a Concave Polyhedral Shell. *ISAS report*, 1975; **40**; 39–60.
- [8] Thill C., Etches J., Bond I., Potter K. and Weaver P., Morphing skins - A review. *The Aeronautical Journal*, 2008; **112**; 117–138.